Supplementary Materials

Fault Activity in Clay Rock Site Candidate of High Level Radioactive Waste Repository, Tamusu, Inner Mongolia

Zheng Rao [1], Guangrong Li [1,*], Xiaodong Liu [1,2], Pinghui Liu [1], Honghui Li [3], Shuai Liu [1], Minqiang Zhu [1], Chao Guo [1], Fengjuan Ni [1], Zhijun Gong [1] and Fiaz Asghar [1]

[1] State Key Laboratory of Nuclear Resources and Environment, East China University of Technology, Nanchang 330013, China; 201800818014@ecut.edu.cn (Z.R.); 198260003@ecut.edu.cn (X.L.); 199560031@ecut.edu.cn (P.L.); 200360016@ecut.edu.cn (S.L.); Zhumq@ecut.edu.cn (M.Z.); 2016070945@ecut.edu.cn (C.G.); 202062003@ecut.edu.cn (F.N.); 201660006@ecut.edu.cn (Z.G.); L2017008103@ecut.edu.cn (F.A.)

[2] Jiujiang University, Jiujiang 332005, China

[3] China Institute for Radiation Protection, Taiyuan, Shanxi 030006, China; lihonghui@cirp.org.cn

* Correspondence: liguangrong0086@ecut.edu.cn

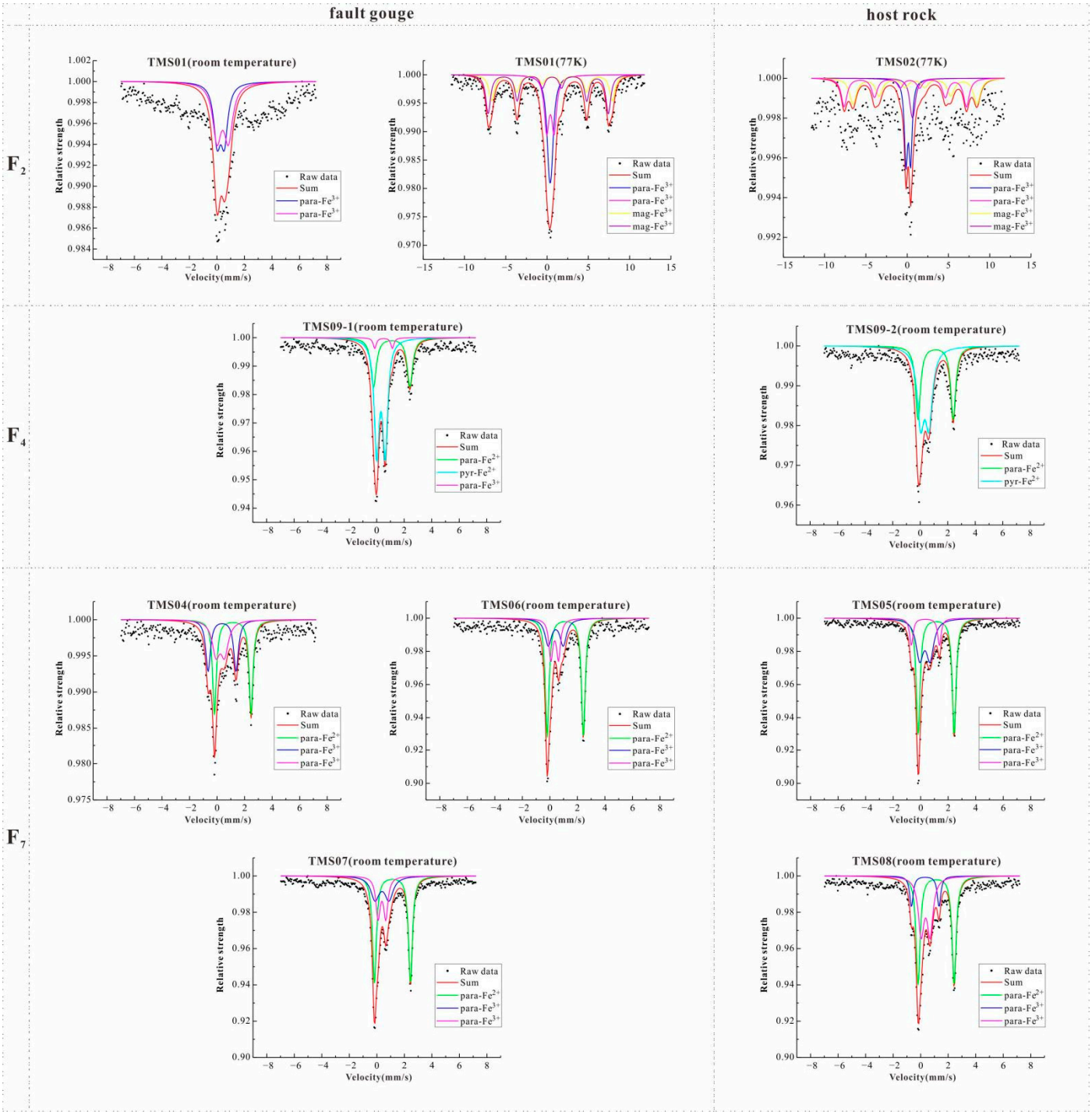

Figure S1. Mossbauer spectroscopy of fault gouge and host rock in Tamusu area.

Table S1. Sample characteristics and sampling location.

Fracture Name	Sample Number	Sampling Location	Sample Characteristics	Sampling Coordinates
F_2	TMS01	Fault zone	Yellowish brown fault gouge	N 40°41'8″ E 103°15'26″
	TMS02	Hanging wall of fault	Yellowish brown medium coarse sandstone	
F_7	TMS04	Fault zone	Incanus fault gouge	N 40°37'15″ E 103°43'38″
	TMS05	Footwall of fault	Incanus medium coarse sandstone	
	TMS06	Fault zone	Incanus fault gouge	
	TMS07	Fault zone	Ash black fault gouge	N 40°37'4″

	TMS08	Hanging wall of fault	Grey medium coarse sandstone	E 103°43'45″
F_4	TMS09-1	Fault zone	Ash black fault gouge	N 40°39'28″
	TMS09-2	Hanging wall of fault	Ash black cloy rock	E 103°32'5″

Table S2. Major element content in fault gouge and host rock.

Fracture Name	F_2		F_7				F_4		
Sample Number	TMS01	TMS02	TMS04	TMS05	TMS06	TMS07	TMS08	TMS09-1	TMS09-2
Lithology	Fault Gouge	Host Rock	Fault Gouge	Host Rock	Fault Gouge	Fault Gouge	Host Rock	Fault Gouge	Host Rock
Al_2O_3	14.22	11.02	11.78	16.45	13.02	14.07	13.64	9.58	12.83
BaO	0.06	0.07	0.02	0.02	0.02	0.02	0.02	0.15	0.03
CaO	0.63	0.63	3.15	2.55	8.93	8.10	8.59	19.00	12.00
Cr_2O_3	<0.01	<0.01	<0.01	<0.01	0.02	<0.01	<0.01	<0.01	<0.01
TFe_2O_3	2.47	0.52	2.31	9.70	7.22	8.26	9.75	7.57	5.08
K_2O	5.61	5.23	2.11	0.86	0.88	1.06	0.33	2.05	2.91
MgO	0.39	0.04	1.14	3.93	4.81	3.71	3.60	5.24	6.09
MnO	0.01	0.01	0.06	0.17	0.14	0.17	0.15	0.17	0.13
Na_2O	2.70	2.04	2.32	4.67	1.77	3.04	3.27	2.60	3.46
P_2O_5	0.14	0.05	0.07	0.21	0.20	0.21	0.21	0.14	0.23
SiO_2	71.20	79.43	72.87	55.63	52.85	50.80	50.86	29.24	38.11
SO_3	0.07	0.10	<0.01	<0.01	<0.01	0.01	<0.01	7.44	1.54
SrO	0.09	0.05	0.03	0.04	0.04	0.04	0.04	0.53	0.11
TiO_2	0.50	0.20	0.33	1.31	1.04	1.23	1.34	0.43	0.57
Loss on ignition	1.60	0.91	3.20	3.74	9.32	9.17	7.81	17.33	16.75

Table S3. carbon and oxygen isotope compositions of fault gouge and host rock.

Fracture Name	Sample Number	Lithology	$\delta^{13}C_{PDB}$(‰)	$\delta^{18}O_{SMOW}$(‰)
F_2	TMS01	Fault gouge	Low carbonate content	
	TMS02	Host rock	−7.9	18.2
F_7	TMS04	Fault gouge	−3.3	9.0
	TMS05	Host rock	−4.1	13.7
	TMS06	Fault gouge	−4.8	10.7
	TMS07	Fault gouge	−5.9	14.9
	TMS08	Host rock	−6.1	11.1
F_4	TMS09-1	Fault gouge	−0.2	22.1
	TMS09-2	Host rock	3.7	28.6

Table S4. Mossbauer parameters and relative contents of various iron species in fault samples from Tamusu area.

Sample Number		Types of Iron Ions	Lithology	Relative Content（%）	IS (mm/s)	QS (mm/s)	HW (mm/s)	Hi (kOe)	Fe^{2+}/Fe^{3+}
F_2	TMS01	para-Fe^{3+}	Fault gouge	45.00 ± 0.86	0.280 ± 0.140	0.520 ± 0.350	0.300 ± 0.210		
		para-Fe^{3+}		55.00 ± 0.87	0.420 ± 0.210	0.830 ± 0.330	0.372 ± 0.092		
	TMS01（77K）	para-Fe^{3+}	Fault gouge	25.00 ± 0.59	0.382 ± 0.032	0.270 ± 0.340	0.350 ± 0.420		
		para-Fe^{3+}		21.00 ± 0.57	0.412 ± 0.058	0.910 ± 0.470	0.350 ± 0.250		
		mag-Fe^{3+}		23.00 ± 0.29	0.590 ± 0.340	0.020 ± 0.380	0.400 ± 0.200	453.2 ± 4.1	
		mag-Fe^{3+}		31.00 ± 0.28	0.370 ± 0.220	−0.460 ± 0.220	0.350 ± 0.140	451.4 ± 2.6	
	TMS02（77K）	para-Fe^{3+}	Host rock	24.00 ± 0.10	0.136 ± 0.081	0.560 ± 0.130	0.229 ± 0.093		
		para-Fe^{3+}		10.00 ± 0.13	0.650 ± 0.300	0.200 ± 0.130	0.340 ± 0.580		
		mag-Fe^{3+}		34.00 ±0.25	0.950 ± 0.200	0.000 ± 0.180	0.500 ± 0.340	465 ± 12	
		mag-Fe^{3+}		32.00 ± 0.22	0.050 ± 0.160	−0.560 ± 0.150	0.420 ± 0.270	459.2 ± 9.8	
F_4	TMS09-1	para-Fe^{2+}	Fault gouge	31.40 ± 0.30	1.097 ± 0.022	2.640 ± 0.043	0.237 ± 0.030		24.641

		pyr-Fe^{2+}		64.70 ± 0.31	0.313 ± 0.008	0.614 ± 0.016	0.214 ± 0.013	
		para-Fe^{3+}		3.90 ± 0.28	0.502 ± 0.076	1.280 ± 0.140	0.140 ± 0.110	
	TMS09-2	para-Fe^{2+}	Host rock	41.60 ± 0.34	1.119 ± 0.015	2.559 ± 0.028	0.213 ± 0.021	
		pyr-Fe^{2+}		58.40 ± 0.32	0.332 ± 0.020	0.599 ± 0.031	0.305 ± 0.031	
		para-Fe^{2+}		42.70 ± 0.38	1.144 ± 0.014	2.657 ± 0.028	0.167 ± 0.018	
	TMS04	para-Fe^{3+}	Fault gouge	28.40 ± 0.66	0.364 ± 0.023	2.030 ± 0.048	0.204 ± 0.043	0.7452
		para-Fe^{3+}		28.90 ± 0.76	0.232 ± 0.069	0.620 ± 0.013	0.330 ± 0.013	
		para-Fe^{2+}		53.70 ± 0.17	1.131 ± 0.005	2.611 ± 0.010	0.164 ± 0.006	
	TMS05	para-Fe^{3+}	Host rock	34.80 ± 0.32	0.306 ± 0.025	0.753 ± 0.052	0.321 ± 0.044	1.1598
		para-Fe^{3+}		11.50 ± 0.24	0.344 ± 0.016	2.039 ± 0.034	0.151 ± 0.031	
		para-Fe^{2+}		56.90 ± 0.30	1.120 ± 0.010	2.628 ± 0.020	0.162 ± 0.011	
F_7	TMS06	para-Fe^{3+}	Fault gouge	23.00 ± 0.13	0.428 ± 0.071	1.090 ± 0.022	0.290 ± 0.100	1.2902
		para-Fe^{3+}		21.10 ± 0.11	0.352 ± 0.029	0.555 ± 0.070	0.174 ± 0.055	
		para-Fe^{2+}		53.20 ± 0.18	1.135 ± 0.007	2.619 ± 0.015	0.169 ± 0.007	
	TMS07	para-Fe^{3+}	Fault gouge	24.00 ± 0.25	0.374 ± 0.053	1.010 ± 0.051	0.366 ± 0.081	1.1367
		para-Fe^{3+}		22.80 ± 0.23	0.370 ± 0.016	0.599 ± 0.066	0.187 ± 0.073	
		para-Fe^{2+}		50.40 ± 0.18	1.126 ± 0.005	2.618 ± 0.010	0.176 ± 0.008	
	TMS08	para-Fe^{3+}	Host rock	12.40 ± 0.21	0.332 ± 0.016	2.006 ± 0.033	0.154 ± 0.028	1.0100
		para-Fe^{3+}		37.20 ± 0.21	0.363 ± 0.014	0.651 ± 0.025	0.252 ± 0.022	

Note: para-Fe^{3+}- paramagnetic ferric iron, para-Fe^{2+}- paramagnetic ferrous iron, mag-Fe^{3+}- iron in magnetite, pyr-Fe^{2+}- ferrous iron in pyrite, IS- isomer shift; QS- quadruple splitting; HW- half width; Hi- hyperfine interactions.

Table S5. Micro morphological classification and relative chronology of quartz in fault gouge.

Structure	**Fracture**	**Denudation**					
	Ru/ Ⅰ$_0$	**Ⅰa**	**Ⅰb**	**Ⅰc**	**Ⅱ**	**Ⅲ**	**Ⅳ**
Conchoidal-like	———						
Subconchoidal-like		———	·····				
Orange peel-like			·····	———			
Squamous-like					———		
Mossy-like					———	·····	
Stalactitic-like						———	
Worm hole-like						———	·····
Pothole-like							———
Cniandai oral-like							———
Age	Holocene	Late Pleisto-cene	Middle Pleistocene	Early Pleistocene		Pliocene	Miocene
		0.01			1		10（Ma）
	Notes：	——— Strong activity		····· Weak activity			

Table S6. Micro morphology type and formation age of quartz grains in fault gouge.

Sample Number	Fracture	Denudation						Fault Name
	Ru/ I_0	Ⅰa	Ⅰb	Ⅰc	Ⅱ	Ⅲ	Ⅳ	
TMS01		▬▬	▪▪▪▪	▪▪▪▪	▬▬	▬▬	▪▪▪▪	F_2
TMS04		▬▬	▪▪▪▪	▬▬	▬▬	▬▬	▪▪▪▪	F_7
TMS06		▬▬	▪▪▪▪	▪▪▪▪	▪▪▪▪	▬▬	▪▪▪▪	
TMS07		▬▬	▬▬	▬▬	▬▬	▪▪▪▪	▪▪▪▪	
Age	Holocene	Late Pleisto-cene	Middle Pleistocene	Early Pleistocene		Pliocene	Miocene	
		0.01			1	10（Ma）		
Notes： ▬▬ Strong activity ▪▪▪▪ Weak activity								